

# Effect of tin content in precursor sols on surface and optical properties of tin incorporated titanium oxide amorphous thin films on glass

Hasmat Khan, Susanta Bera, Saswati Sarkar and Sunirmal Jana\*

Sol-Gel Division, CSIR-Central Glass and Ceramic Research Institute (CSIR-CGCRI)

196 Raja S.C. Mullick Road, P.O. Jadavpur University, Kolkata 700 032, West Bengal, India

\*Corresponding author: Tel.: +91 33 2473 3496, Extn. 3303; Fax: +91 33 2473 0957 E-mail: sjana@cgcri.res.in, janasunirmal@hotmail.com

**Abstract—** In this work, adopting simple sol-gel dip coating technique, we deposited tin incorporated amorphous titanium oxide thin films (thickness,  $152\pm2$  nm) on pure silica glass from precursor sols (viscosity,  $7.5\pm1.5$  cP) with a fixed metal oxide content (six weight percent) by varying tin (II) ethyl hexanoate to titanium isopropoxide molar proportions,  $R$  (0 to 0.18) in presence of acetylacetone as sol stabilizer. The films cured at  $450^{\circ}\text{C}$  in air atmosphere were found to be highly transparent in the visible region and X-ray amorphous. The samples were characterized by spectroscopic ellipsometer for the measurement of physical thickness, refractive index (RI) and extinction co-efficient ( $k$ ) while the volume porosity was calculated from the measured RI of the films. With increasing tin content in the precursor sols, the root means square surface roughness (RMSSR) as measured from atomic force microscope found increased while the RI decreased but the trend in change of RMSSR found identical with the trend in change of volume porosity and extinction co-efficient of the films. In brief, the RMSSR was found to be closely related to  $k$  and volume porosity as well as RI of the films. A co-relation was also drawn between the RMSSR values with the static water contact angle on the surface of the films. Amorphous metal oxide thin films with relatively high refractive index, transparent and low optical loss could be used as optical waveguide materials. Therefore, the film (TS3) deposited from the precursor sol with  $R$ , 0.03 showed highest RI value (1.86) with lowest RMSSR and  $k$  values. This TS3 film could be used as planar optical waveguide material.

**Keywords—** Sol-gel dip coating, amorphous thin film, surface roughness, ellipsometric analysis, static water contact angle

## I. INTRODUCTION

Amorphous metal oxide semiconductor based transparent thin films have attracted a great scientific interest for their amazing properties and applications in diverse areas such as optical waveguides, couplers, resonators, etc. [1]-[3]. The properties of the films could further be enhanced if proper mixed oxide with optimized composition be used [4]. On the other hand, the thin film materials as photonic materials with high refractive index and low optical loss with low surface

roughness are mostly desired for fabrication optical waveguide [5].

On the other hand, transparent high refractive indexed metal oxide thin film materials including zirconia, titania, tantalum oxide are well studied in recent years for the development of optical waveguides [6]. It is known that the light propagation losses in amorphous materials are generally low compare to their crystalline counterparts [6]. Among the several metal oxides, titania is a wide band gap (3.2 eV) semiconductor that shows good durability, high transmittance and refractive index (RI) over the visible region [7]-[9]. In the same vein, amorphous titanium oxide shows low propagation loss of 7.5 dB/cm at around 633 nm and 1.2 dB/cm at  $\sim$ 1550 nm whereas the loss of anatase titania is 5.8 dB/cm at 1550 nm [10]-[11]. There are several techniques for deposition of titanium oxide including cost effective and facile sol-gel technique and it is found that the optical properties of sol-gel based titanium oxide film depend on the precursor sol/solution composition and chemistry, incorporation/doping of foreign metal, film curing atmosphere and temperature etc. [12]. Among the several reports available in the literature, Bsiri et al. [13] fabricated chromium doped densified titanium thin films with high refractive index. Also, Mahanty et al. [14] reported crystalline tin doped titanium oxide powder with improved optical properties. However, to the best of our knowledge, the sol-gel preparation of amorphous tin incorporated titanium oxide thin films with relatively high refractive index, low optical loss and low surface roughness is yet to be found in the literature.

In this work, we report the successful development of amorphous tin incorporated titanium oxide (TS) thin films with relatively high refractive index, low optical loss in terms of low extinction coefficient and low surface roughness by adopting sol-gel technique using the optimized precursor composition through finding out from varying molar proportions,  $R$  (0 to 0.18) of Sn(II)-ethyl hexanoate (TEH) to titanium (IV) isopropoxide (TIOT). It was seen that with increasing tin content in the precursor sols, the root means square surface roughness (RMSSR) found increased

while the RI decreased but the trend in change of RMSSR found identical with the trend in change of volume porosity and extinction co-efficient of the films. Therefore, the co-relations have been drawn between the RMSSR values with the RI, extinction co-efficient, volume porosity and the static water contact angle on the surface of the films as functions of  $R$  through several adequate characterizations. Finally, we found that the film derived from the optimized sol composition with  $R = 0.03$  was the best to be used as an optical waveguide material.

## II. EXPERIMENTAL

### A. Preparation of Precursor Sols

Initially, titanium (IV) isopropoxide (TIOT) was dissolved in mixed solvents (1:1, v/v) medium containing ethanol (EMSURE<sup>®</sup>, Merck, Germany) and 2-butanol (E. Merck, 99%). After 5 min of stirring, acetylacetone (acac; Merck, 99%) was added to the above aliquot as stabilizer (TIOP : acac = 1.5, molar ratio) and continued the stirring for another 5 h to obtain a cleared pristine sol. This pristine sol was then divided into five equal parts (each having 100 ml in volume). In the next, different amount of Sn(II)-ethyl hexanoate (TEH) (Sigma-Aldrich, 95%) was added into the five parts of the pristine sol by varying TEH to TIOT molar proportions ( $R$ ); 0, 0.03, 0.06, 0.11 and 0.18 during vigorously stirring for approximately 5 h. The sols with varying  $R$  values of 0, 0.03, 0.06, 0.11 and 0.18 were designated as TS0S, TS3S, TS6S, TS11S and TS18S, respectively. Finally, the required amount of the mixed solvents was added in each of the precursor sol to make the total mixed metal oxide content fixed to six weight percent in each sol with continuous stirring. It is noted that during the preparation of precursor sols, the room relative humidity was maintained within 45 to 50%.

### B. Thin Film Deposition

As-prepared sols could not produce homogeneous coating on cleaned and polished silica glass substrate (Quartz glass plate, code CUSQ223; Ants Ceramics Pvt. Ltd., India; dimension: length 75 mm, width 25 mm and thickness 1 mm). However, after 24 h of ageing, the aged sols were found to be useful as wettable sols for the formation of thin films on the substrate by dip coating technique (Dip Master 200, Chemat Technology Inc., USA). All the films were deposited with a fixed withdrawal speed of 18 cm/min and after the deposition; the as-coated films were initially baked at 150°C for about 30 min in an air oven followed by final curing at 450°C with a soaking period of 1 h in the same air oven. The final films were designated as TS0, TS3, TS6, TS11 and TS18 that derived from the precursor sols of TS0S, TS3S, TS6S, TS11S and TS18S, respectively.

## III. CHARACTERIZATIONS

The amorphous nature of the films was confirmed from X-ray diffraction (XRD) patterns of the films, recorded by employing Bruker make D8 Advance with DAVINCI design X-ray diffraction unit having nickel-

filtered CuK $\alpha$  radiation source (wavelength = 1.5418 Å) in the 2 $\theta$  range of 10° to 80°. The FTIR vibrations of the scratched off film materials were measured by the spectrometer (Nicolet 5700, Thermo Electron Corporation) with the number of scans of 100 and the wavenumber resolution of 4 cm $^{-1}$ . Viscosity (7.5±1.5 cP) of aged precursor sols was measured at room temperature (~30°C) by software controlled Thermo Scientific HAKKE Rheostress (model RS6000), Germany using cone-plate (sensor system, C60/1) at a shear rate and time, 400 S $^{-1}$  and 60S, respectively. The film physical thickness (T) and refractive index (RI) were measured using a Spectroscopic Ellipsometer (Semilab, 1117 Budapest, Hungary, model GES5-E) in the wavelength region of 300 to 1000 nm. The dispersion curves (i.e. RI versus wavelength plots) were derived with help of the available software of the instrument using Cauchy-Lorentz model. It is worthy to note that the T and RI values of each film were determined at 632.8 nm and the data is displayed in Table 1. Atomic force microscope (AFM, Nanosurf Easy Scan 2, Switzerland) was used to analyze the film surface topography as well as average line scan profile height whereas the root means square (RMS) surface roughness were determined from the AFM images (dimension: 50 μm x 50 μm) [15] of the thin films employing WSxM 5.0 Develop 7.0-Image Browser software. UV-Vis-NIR spectrophotometer (Shimadzu UV-PC-3100; photometric accuracy: transmission ±0.3%, wavelength resolution, 0.10 nm) was used to measure the transmittance property of the films in UV-visible regions. Static water contact angles (WCA) on the surface of the films were measured at room temperature by using Easy drop (Krüss) FM 40MK2 GmbH, Hamburg, Germany.

## IV. RESULTS AND DISCUSSION

### A. X-ray Diffraction Study

X-ray diffraction patterns of TS films along with pristine titanium oxide film are shown in Figure 1. It can be seen from the figure that all the films are X-ray amorphous. A broad XRD peak in the 2 $\theta$  region of ~25° to ~28° was found, implying the amorphous nature of the films.

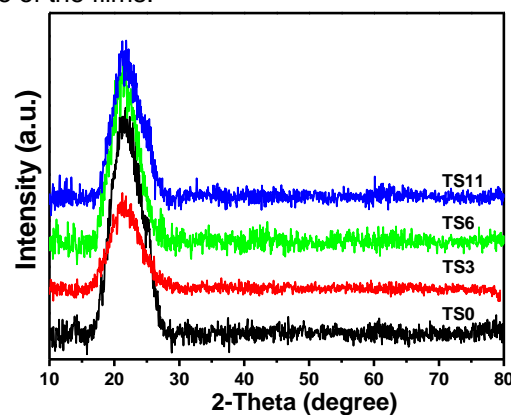


Fig.1. XRD patterns of the films cured at 450°C in air atmosphere.

### B. Film Surface Property

Film surface feature (Fig. 2) and surface roughness were analysed by AFM studies. In this respect, the root mean square surface roughness values (RMSSR) was calculated from the respective AFM images with a fixed scan area of  $50 \mu\text{m}^2$  using WSxM 5.0 Develop 7.0-Image Browser software. It was observed that the RMSSR (Table 1) was found to be increased with increasing TEH to TIOT molar proportions ( $R$ ) in the precursor sols. However, the TS18 film derived from the precursor sol with  $R$ , 0.18 showed extremely high RMSSR value. It is known [15] that the RMSSR ( $R_q$ ) of a material surface could be related to root mean square average of the roughness profile coordinates. The  $R_q$  could be expressed (eqn. 1) [15] in terms of the evaluation length,  $L$  having the profile coordinates  $Z$  and  $X$ . In this work, we determined the  $Z$  from the line scan profile height of AFM images of the films (thickness,  $152 \pm 2$  nm, Table 1). On the other hand, the surface roughness of sol-gel based film could depend upon several factors such as surface roughness of substrate used, film thickness, film homogeneity, composition of precursor sol, growth of crystalline materials etc. [16]-[17]. It is worthy to note that in the present work, all the films were amorphous in nature with nearly similar physical thickness (Table 1) and we used silica glass substrate of similar surface roughness value (0.75 nm) for deposition of all the films. Therefore, the increased surface roughness could mostly be associated with the composition of the precursor sol where the change of  $R$  value could be the major influential factor. However, the exact reason for the influence of  $R$  was difficult to understand at the present work and it will be the future scope of work.

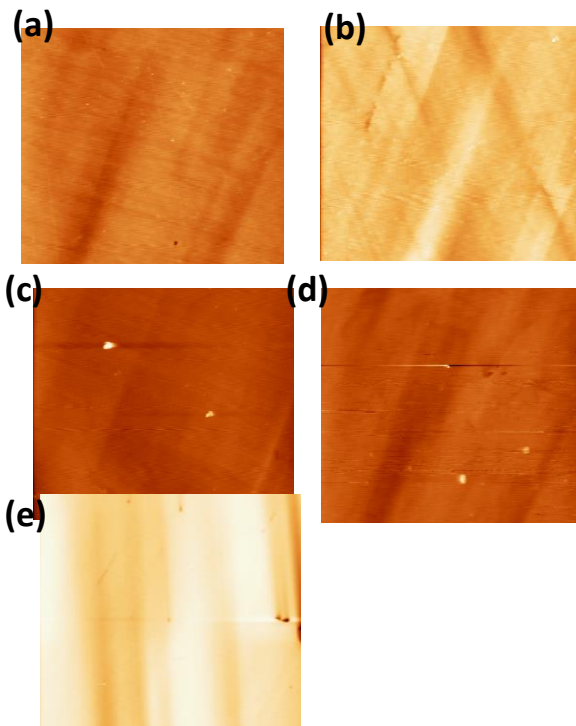


Fig.2. AFM images of (a) TS0, (b) TS3, (c) TS6, (d) TS11 and (e) TS18.

$$R_q = \sqrt{\frac{1}{L} \int_0^L |Z^2(x)| dx} \quad \dots \quad (1)$$

In eqn. 1,  $Z(x)$  is the function that demonstrates the surface profile. The profile of the sample could be analyzed in terms of profile height ( $Z$ ) and position ( $x$ ) for the evaluation length,  $L$ .

Table 1: Characteristics of precursor sols and thin films

Film designation	Film thickness ( $\pm 2$ nm)	Refractive index ( $\pm 0.01$ )	Extinction coefficient, $k$ ( $\pm 0.0002$ )	Volume porosity, $P$ ( $\pm 0.5\%$ )	RMS roughness (nm)	Average H (nm)	WCA ( $\pm 1^\circ$ )
TS0	154.3	1.77	0.0078	20.20	2.4	21.11	55
TS3	149.7	1.86	0.0045	13.49	1.8	19.59	52
TS6	150.3	1.83	0.0061	15.67	2.2	20.35	54
TS11	154.7	1.81	0.0078	17.16	2.9	23.57	57
TS18	150.9	1.72	0.0105	24.15	13.3	128.79	66

Note: RMS, H and WCA indicate root means square, atomic force microscopic line scan profile height and static water contact angle on the thin film surface, respectively.

### C. FTIR Spectral Study

FTIR spectral study (Fig. 3) was carried out systematically to reveal IR active bond vibrations that would originate from various functional groups and metal oxygen bonds in the sample scratched off from as-deposited TS11 and the  $450^\circ\text{C}$  cured thin films, could address the formation of amorphous oxide thin films derived from the precursor sols. The FTIR vibrations of the as-deposited sols to oxide (TS) films could suggest that different organic functional groups such as metal acetylacetone complex were present till the film curing temperature of  $\leq 150^\circ\text{C}$  (Fig. 3a). The assignment of appeared vibration peaks that found in as-prepared TS15 film is given in Table 2.

Table 2. Assignment of FTIR vibrations

FTIR vibrations ( $\text{cm}^{-1}$ )	Assignments	References
3600-3100	$\nu_{\text{O-H}}$	18
1720	$\nu_{\text{COOH}}$ (free 2 ethyl hexanoic acid)	19
1590	$\nu_{\text{C=O}}$ + $\nu_{\text{C=C}}$ (asymmetric acetylacetone)	20
1530	$\nu_{\text{C=C}} + \delta_{\text{CH}}$ (acetylacetone)	20
1380	$\delta_{\text{s}}$ ( $\text{CH}_3$ )	20
1150	$\nu$ ( $\text{CH}_2$ bending)	20
450-700	$\nu_{\text{Sn-O}}/\nu_{\text{Ti-O}}$	21

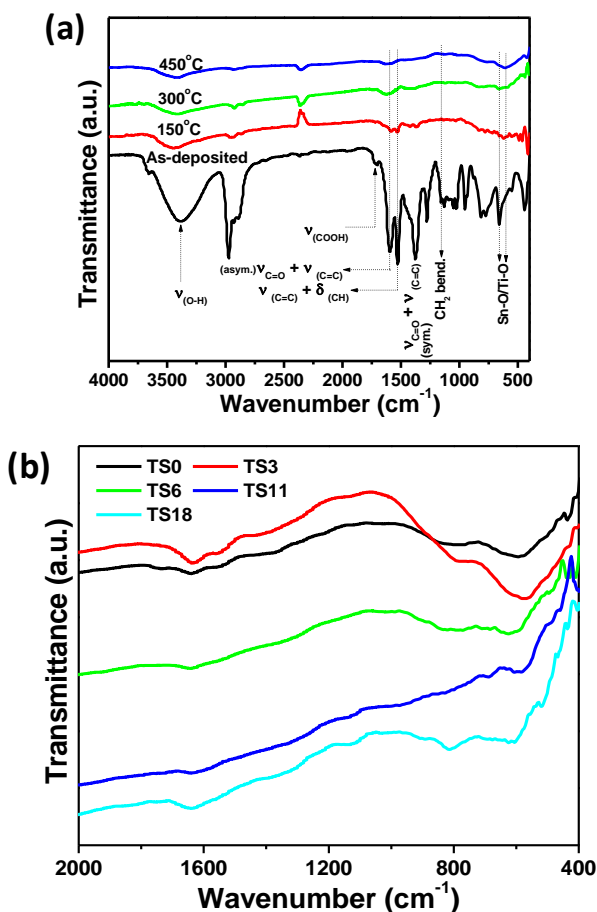


Fig. 3. Substrate corrected FTIR spectra of scratched off titanium tin oxide thin film materials: (a) TS11 as-coated film cured at different temperatures and (b) TS thin film materials cured at 450°C.

On the other hand, the FTIR spectra of 450°C cured TS thin films materials was also performed (Fig. 3b). In TS0 thin film, a broad vibration ranging from 700 to 450 cm<sup>-1</sup>, centered at ~600 cm<sup>-1</sup> was appeared, could be attributed to Ti-O vibration [21]. Upon incorporation of tin into the precursor sols for TS thin films, new vibration peaks were appeared (such as ~520 cm<sup>-1</sup>, ~570 cm<sup>-1</sup>, ~680 cm<sup>-1</sup>). It is worthy to note that the presence of Sn-O-Sn vibrations in the TS films might be overlapped within the broad vibration of Ti-O. However, with increasing the incorporation level of tin, the relative intensity of the new peaks systematically increased. This result could imply the formation of hetero atomic linkage Ti-O-Sn along with homo atomic linkage of Ti-O-Ti/Sn-O-Sn.

#### D. Optical Property

Refractive index (measured at 632.8 nm) and physical thickness of the films cured at 450°C temperature are given in Table 1. From the measured refractive index, it could possible to calculate the volume porosity, P in percentage (%) of the TS thin films using Lorentz-Lorentz (L-L) relationship (eqn. 2) [15].

$$1 - (P/100) = (n^2 - 1) / (N^2 - 1) \times (N^2 + 2) / (n^2 + 2) \quad (2)$$

where, 'N' corresponds to the RI of pure dense material and 'n' is the observed RI of the film.

Using eqn. 2, the calculated volume porosity, P (%) from ellipsometrically measured refractive index values of TS0, TS3, TS6, TS11 and TS18 thin films cured at 450°C were found to be ~20.2, ~13.5, ~15.7, ~17.2 and ~24.2, respectively (Table 1). It is noted that the calculation of P was based [22] on the refractive index (N, 2.064 at 632.8 nm) of dense titania and the experimentally measured RI (n) values of the TS films. In this work, among all the films, TS3 showed the lowest volume porosity that could possibly be due to greater densification of the film matrix [13]. This assumption could be justified from the highest refractive index of TS3 film. In this respect, the film showed lowest RMSSR that could have a weak scattering effect on light during the measurement of refractive index (RI) using spectroscopic ellipsometer

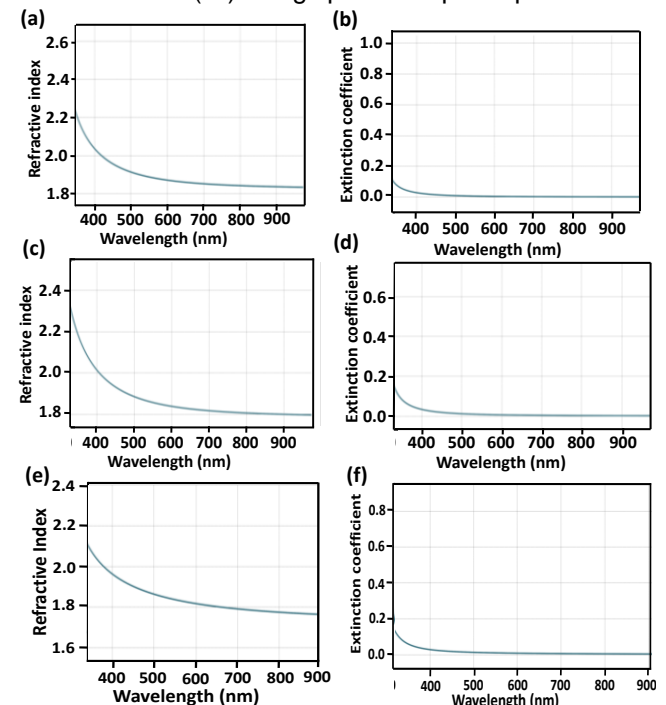


Fig. 4. Plots of refractive index as function of wavelength (optical dispersion curves; a, c and e for TS3, TS6 and TS11, respectively) and plots of extinction coefficient as function of wavelength (b, d and f for TS3, TS6 and TS11, respectively)

and as a result, the measured RI was relatively high [23]. On the other hand, the maximum volume porosity of TS18 film could be related to its lowest refractive index of the film. It is worthy to note that the dense tin dioxide has the comparable refractive index (2.006) [24] with titanium dioxide. In this case, all the composite film should show similar refractive index but it was seen that with increasing tin content in the precursor sols, the RI of the developed films was found to be decreased and the calculated volume porosity was noticed to be increased.

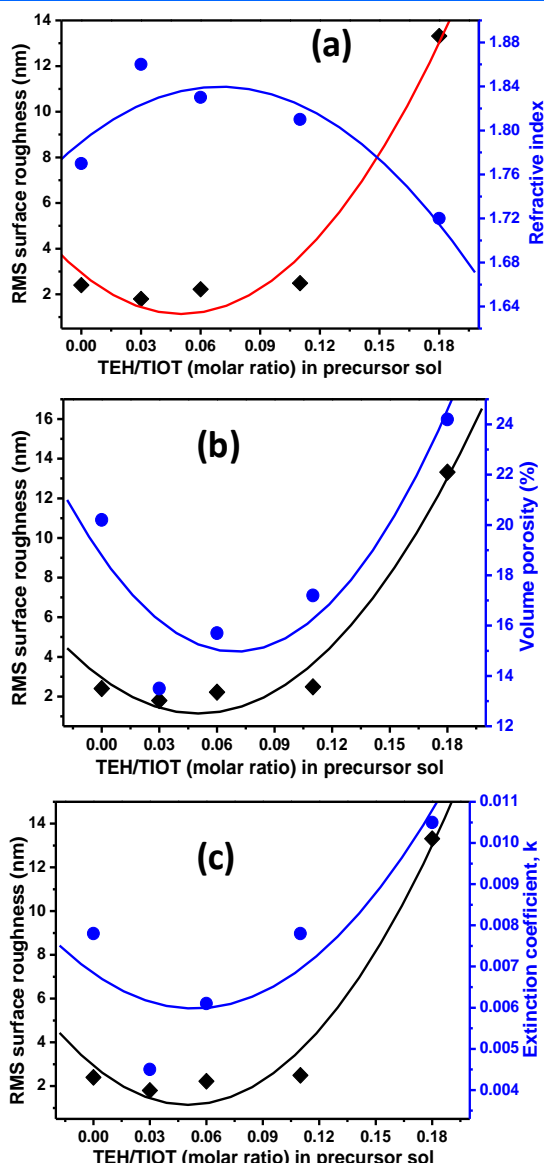


Fig. 5. (a) Plots of RMSSR and RI, (b) plots of RMSSR and volume porosity and (c) plots of RMSSR and extinction coefficient as a function of  $R$ .

To verify the above argument, we calculated volume porosities from the measured refractive indices at 832.8 nm of the thin films. However, it was observed that upon incorporation of tin into the precursor sols forming TS thin films, initially, the refractive index was found to be increased significantly and then, it became gradually decreased and the TS3 showed maximum refractive index (~1.86) even compare to pristine titanium oxide thin film (~1.77). This result fully supported the calculated volume porosity of the samples. It is worthy to note that all the films including TS3 film was amorphous. On the other hand, among all the films, TS3 showed lowest extinction coefficient value indicating low absorption (attenuation) loss particularly at 632.8 nm as per the linear relationship [25] (eqn. 3) that observed between the measured extinction and absorption coefficients. It is noted that we measured (Fig. 4) the dispersion curves i.e. the change of RI and the change of extinction coefficient as a function of wavelengths starting from UV to NIR

regions (350 nm to 950 nm) for understanding the change of optical constants of the TS films.

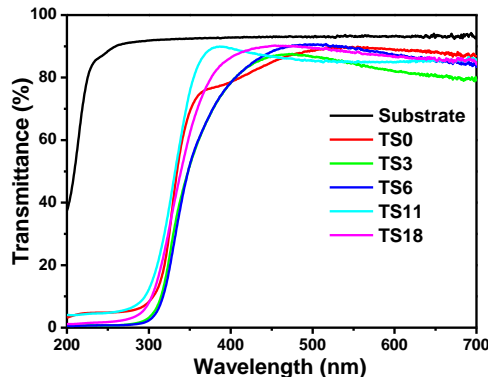


Fig. 6. UV-Visible transmittance spectra of TS thin films.

The plot (Fig. 5a) of change of RMS roughness with refractive index as a function of  $R$  values in the precursors shows an approximately inverse relationship with the RI and the RMS roughness changes. In the same vein, the plot (Fig. 5b) of change of RMSSR with volume porosity as a function of tin content also reveals similar relationship of the measured RI with the RMS roughness values of the films. However, approximately similar nature (Fig. 5c) was observed between the changes of extinction coefficient with volume porosity as function of tin content in the precursor sols. This result suggested that the volume porosity/surface roughness could control the attenuation loss of the films visa-a-vis the refractive index change of the TSO thin films as both the metal oxides possess similar RI values in their densified crystalline structures [24].

$k = \alpha\lambda/4\pi$  - - - (3), where  $\alpha$  and  $\lambda$  are absorption coefficient and wavelength of light, respectively)

UV-Visible transmission spectra of the films on pure silica glass substrate are shown in Figure 6. The percent (%) transmittance of the films in the visible region was found ~80%. However, a slightly lower transmittance was noticed for the TS3 film compared to other films i.e. TS0, TS3, TS6, TS11 and TS18 films. This could attribute to the relatively high film refractive index that could induce a higher reflectivity of TS3 film [15]. Therefore, the TS3 film with high refractive index with low optical loss and low optical loss in terms of extinction coefficient could be useful as planar waveguide material [15].

#### E. Static Water Contact Angle

Surface property in terms of RMSSR was validated by measuring static water contact angle (WCA) of the TS films at room temperature. Figure 7 shows the images of water-droplets onto the surface of the TS thin films. It was observed that with increasing Sn content of the precursor sols, the WCA was found to be increased and a maximum value of WCA was found in TS18 film which showed the highest RMSSR. It is noted that the surface roughness of the films could play an important role upon the surface property in

terms of WCA of the films [15]. In the present work, on increasing the Sn content in the precursor, the trend of change of RMSSR and the change of measured WCA showed similar behaviour that fully supported the change of film surface property in terms of RMSSR of the TS film (Fig. 7).

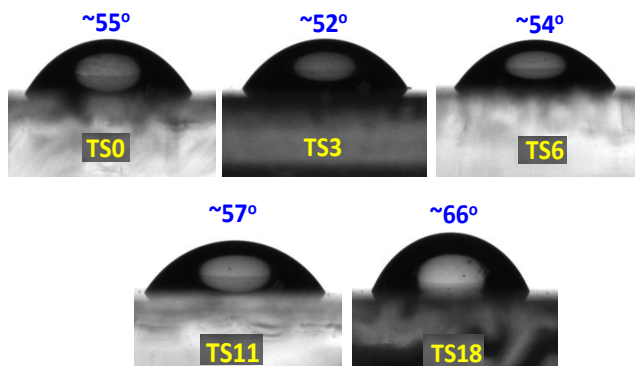


Fig.7. Photographs showing the change in shape of water-droplets on the surfaces of TS thin films (static water contact angles in degrees are embedded in the respective figures).

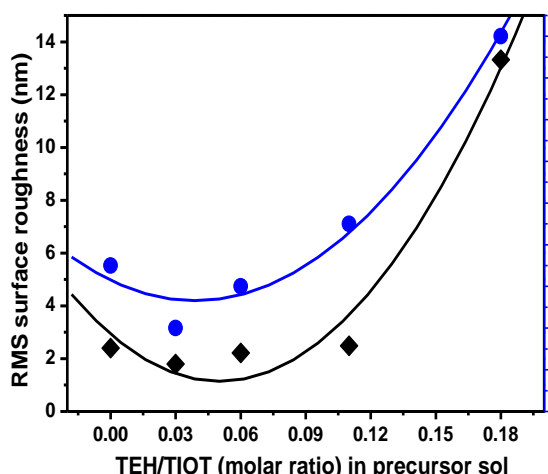


Fig. 8. Plots of RMSSR and static water contact angle as a function of  $R$ .

## V. CONCLUSION

Adopting simple sol-gel dip coating technique, we deposited tin incorporated amorphous titanium oxide thin films (thickness,  $152\pm2$  nm) on pure silica glass from precursor sols (viscosity,  $7.5\pm1.5$  cP) with a fixed metal oxide content (6 weight percent) by varying tin (II) ethyl hexanoate to titanium isopropoxide molar proportions,  $R$  (0 to 0.18) in presence of acetylacetone as sol stabilizer. The films cured at  $450^{\circ}\text{C}$  in air atmosphere were found to be highly transparent in visible region and was X-ray amorphous. With increasing tin content in the precursor sols, the root means square surface roughness (RMSSR) found to be increased while the RI decreased but the trend in change of RMSSR found identical with the trend in change of volume porosity and extinction co-efficient of the films. A co-relation was also found between the RMSSR values with the static water contact angles on

the surface of the films. The amorphous metal oxide thin film (derived from the precursor sol with  $R = 0.03$ ) with relatively high refractive index, highly transparent and low optical loss could be used as optical waveguide materials.

## VI. ACKNOWLEDGEMENT

The authors wish to acknowledge the Director, CSIR-CGCRI, Kolkata for his kind permission to publish this work. The authors also acknowledge the help rendered by Analytical Facility Division for XRD characterization. The work has been done under CSIR funded Supra Institutional Network Project (SINP) (No. ESC0202) of 12<sup>th</sup> Five Year Plan.

## VII. REFERENCES

- [1] J. Socratus , K. K. Banger , Y.Vaynzof , A. Sadhanala, Adam D. Brown , A. Sepe , U. Steiner , and H. Sirringhaus "Electronic Structure of Low-Temperature Solution-Processed Amorphous Metal Oxide Semiconductors for Thin-Film Transistor Applications" *Adv. Funct. Mater.* Vol. 25, pp.1873–1885, March 2015.
- [2] R. Nayak, V. Gupta, A.L Dawar, K. Sreenivas, Optical waveguiding in amorphous tellurium oxide thin films. *Thin Solid Films* vol. 445, pp. 118–126, November 2003.
- [3] L. Bi, J. Hu, P. Jiang, D. H. Kim, G. F. Dionne, L. C. Kimerling, and C. A. Ross, "On-chip optical isolation in monolithically integrated non-reciprocal optical resonators," *Nat. Photonics* vol. 5, pp. 758–762, September 2011.
- [4] J. Yu, X. Zhao, Q. Zhao, G. Wang "Preparation and characterization of super-hydrophilic porous  $\text{TiO}_2$  coating films" *Mater. Chem. Phys.* vol. 68 pp. 253–259, 2001.
- [5] B. Guha, J. Cardenas, and M. Lipson, "Athermal silicon microring resonators with titanium oxide cladding," *Opt. Express* vol. 21, pp.26557–26563, October 2013.
- [6] R. Olshansky, "Mode Coupling Effects in Graded-index," *Opt. Fibers. Appl. Opt.* Vol. 14, No. 4, 935-945 April 1975.
- [7]. P. Rabiei, J. Ma, S. Khan, J. Chiles, and S. Fathpour, "Submicron optical waveguides and microring resonators fabricated by selective oxidation of tantalum," *Opt. Express*, vol. 21, pp. 6967–6972 February 2013.
- [8]. J. D. B. Bradley, C. C. Evans, J. T. Choy, O. Reshef, P. B. Deotare, F. Parsy, K. C. Phillips, M. Lončar, and E. Mazur, "Submicrometer-wide amorphous and polycrystalline anatase  $\text{TiO}_2$  waveguides for microphotonic devices," *Opt. Express* vol. 20, pp. 23821–23831, October 2012.
- [9] G. E. Jellison, Jr., L. A. Boatner, J. D. Budai, B.-S. Jeong, and D. P. Norton, "Spectroscopic ellipsometry of thin film and bulk anatase ( $\text{TiO}_2$ )," *J. Appl. Phys.* Vol. 93, pp. 9537, January 2003.
- [10] O. Reshef, K. Shtyrkova, M. G. Moebius, S. Griesse-Nascimento, S. Spector, C. C. Evans, E.

- Ippen, and E. Mazur, "Polycrystalline anatase titanium dioxide microring resonators with negative thermo-optic coefficient," *J. Opt. Soc. Am. B*, vol. 32, pp. 2288–2293, 2015.
- [11] F. Jiang, L.Bi, H.Lin, Q.Du, J.Hu, A.Guo, C. Li, J. Xie, and L. Deng, "Microstructure, optical properties, and optical resonators of  $Hf_{1-x}Ti_xO_2$  amorphous thin films," *Opt. Mater. Express*, Vol. 6, pp. 1872, 2016
- [12] M. Pal, S. Bera, S. Jana, "Effect of precursor sol pH on microstructural, optical and photocatalytic properties of vacuum annealed zinc tin oxide thin films on glass," *J. Sol-Gel Sci. Technol.* vol. 67, pp 8–17, July 2013.
- [13] N. Bsiri, M.A. Zrir, A. Bardaoui, M. Bouaïcha, "Morphological, structural and ellipsometric investigations of Cr doped  $TiO_2$  thin films prepared by sol-gel and spin coating," *Ceramics International* vol. 42 pp. 10599–10607, March 2016.
- [14] S. Mahanty, S. Roy, S. Sen, "Effect of Sn doping on the structural and optical properties of sol-gel  $TiO_2$  thin films," *J. Cryst. Growth*. vol. 261 pp. 77–81, 2004 September.
- [15] S. Sarkar, S. K. Bhadra, and S. Jana, "Fabrication, characterization and water wetting behavior of mesoscale 1D/2D periodic structured silica-zirconia sol-gel thin films," *RSC Adv.* vol. 6, pp. 46048-46059, April 2016.
- [16] S. Dhanapandian, A. Arunachalam, C. Manoharan, "Highly oriented and physical properties of sprayed anatase Sn-doped  $TiO_2$  thin films with an enhanced antibacterial activity," *Appl Nanosci* vol. 6, pp. 387–397, April 2016.
- [17] A.V. Manole, M. Dobromir, M. Gîrtan, R. Mallet, G. Rusu, D. Luca, "Optical properties of Nb-doped  $TiO_2$  thin films prepared by sol-gel method," *Ceramics International* vol. 39 pp. 4771–4776, November 2013.
- [18] A. Lenz and L. Ojamäe, "Theoretical IR Spectra for Water Clusters ( $H_2O$ ) $n$  (n = 6-22, 28, 30) and Identification of Spectral Contributions from Different H-Bond Conformations in Gaseous and Liquid Water," *J. Phys. Chem. A* vol. 110, pp. 13388-13393, September 2006.
- [19] S. K. Papageorgiou, E. P. Kouvelos, E. P. Favvas, A. A. Sapalidis, G. E. Romanos, F. K. Katsaros, "Metal-carboxylate interactions in metal-alginate complexes studied with FTIR spectroscopy," *Carbohydr. Res.* vol. 345 pp. 469–473, December 2010.
- [20] S. K. Sarkar, J. Y. Kim, D. N. Goldstein, N. R. Neale, K. Zhu, C. M. Elliott, A. J. Frank, S. M. George, " $In_2S_3$  Atomic Layer Deposition and Its Application as a Sensitizer on  $TiO_2$  Nanotube Arrays for Solar Energy Conversion," *J. Phys. Chem. C* vol. 114, pp. 8032–8039, March 2010.
- [21] E. H. de Faria, A. L. Marçal, E. J. Nassar, K. J. Ciuffi, P. S. Calefi, "Sol-Gel  $TiO_2$  Thin Films Sensitized with the Mulberry Pigment Cyanidin," *Mater. Res.* vol. 10, pp. 413-417, November 2007.
- [22] S. Sarkar, R. D. Roy, P. K. Biswas, S. K. Bhadra and S. Jana, "Mesoscale Surface Patterned Silica-Titania Sol-Gel Thin Film on Glass," *International J. Eng. Innovative Technol.* vol. 3, pp. 212-218, April 2014.
- [23] J. Jaiswal, A. Sanger, A. Kumar, S. Mourya, S. Chauhan, R. Daipuriya, M. Singh and R. Chandra, "Enhanced Optical Absorbance of Hydrophobic Ti Thin Film: Role Of Surface Roughness," *Adv. Mater. Lett.* vol. 7, pp. 485-490, March 2016.
- [24] P. Patnaik, "Hand Book of Inorganic Chemicals," The Mc Graw-Hill Companies, 2003, New York.
- [25] R. Vinodkumar, I. Navas, K. Porsezian, V. Ganesan, N. V. Unnikrishnan, V. P. M. Pillai, "Structural, spectroscopic and electrical studies of nanostructured porous  $ZnO$  thin films prepared by pulsed laser deposition," *Spectrochimica Acta Part A: Molecular and Biomolecular Spectroscopy* vol. 118, pp. 724–732, January 2014.